

UDC 548.73:547.13:546.73

**UNUSUAL LAYER STRUCTURE IN AN ION-PAIRED COMPOUND  
CONTAINING TETRA(ISO thiOCYANATE)COBALT(II) DIANION  
AND 4-NITROBENZYL PYRIDINIUM:  
CRYSTAL STRUCTURE AND MAGNETIC PROPERTIES**

**H.-Q. Ye, Y.-Y. Li, R.-K. Huang, X.-P. Liu, W.-Q. Chen, J.-R. Zhou, L.-M. Yang, C.-L. Ni**

*Department of Applied Chemistry, Institute of Biomaterial, College of Science, South China Agricultural University, Guangzhou, P. R. China*

E-mail: scauchem534@126.com (J.-R. Zhou)

*Received January, 12, 2013*

A new ion-paired compound  $[4\text{NO}_2\text{BzPy}]_2[\text{Co}(\text{NCS})_4]$  (**1**) ( $[\text{4NO}_2\text{BzPy}]^+ = 1\text{-}(4'\text{-nitrobenzyl})\text{pyridinium}$ ,  $\text{NCS}^- = \text{isothiocyanate}$ ) is synthesized and characterized by elemental analysis, IR and UV-Vis spectra, ESI-MS and single crystal X-ray diffraction. Compound **1** is orthorhombic, space group  $Pbcn$ , with  $a = 13.188(2)\text{\AA}$ ,  $b = 8.458(1)\text{\AA}$ ,  $c = 29.281(4)\text{\AA}$ ,  $V = 3266.2(7)\text{\AA}^3$ ,  $D_{\text{calcd}} = 1.468\text{ g/cm}^3$ ,  $Z = 4$ ,  $F(000) = 1476$ ,  $R_1 = 0.0332$ . The  $[\text{Co}(\text{NCS})_4]^{2-}$  anions form an unusual layer structure by  $\text{S}\cdots\text{N}$  and  $\text{S}\cdots\text{Co}$  interactions, while the  $[\text{4NO}_2\text{BzPy}]^+$  cations stack into a 1D column by the  $p\cdots\pi$  stacking interaction in the solid state of **1**. A magnetic measurement in the range 2–300 K shows a weak antiferromagnetic exchange with  $\theta = -2.42\text{ K}$  in **1**.

**К e y w o r d s:** 1-(4'-nitrobenzyl)pyridinium, tetra(isothiocyanate)cobalt(II) anion, layer structure, magnetic properties.

Non-covalent bonding interactions such as hydrogen bonding, ion-ion interactions, ion-dipole interactions,  $\pi-\pi$  interactions, dipole-dipole interactions, and van der Waals forces play a major role in the self-assembly of large molecules, crystal packing, and biological pattern recognition [1–4]. Intensive structural investigations in the fields of metal-ligand compounds have shown that these weak forces are ubiquitous and, to a vast extent, lead to the formation of their 1D, 2D, and 3D structures [5–10]. In some ion-pair compounds containing  $[\text{Ni}(\text{dmit})_2]^-$  ( $\text{dmit}^{2-} = 2\text{-thioxo-1,3-dithiole-4,5-dithiolate}$ ) [11],  $[\text{M}(\text{mnt})_2]^{n-}$  ( $\text{M} = \text{Ni}^{3+}$ ,  $\text{Pd}^{3+}$ ,  $\text{Pt}^{3+}$ ,  $\text{Cu}^{2+}$ ;  $\text{mnt}^{2-} = \text{maleonitriledithiolate}$ ;  $n = 1$  or 2) [12–15],  $[\text{M}(\text{CN})_6]^{n-}$  ( $\text{M} = \text{Co}^{3+}$ ,  $\text{Cr}^{3+}$ ,  $\text{Fe}^{2+}$ ,  $\text{Fe}^{3+}$ ,  $\text{Mn}^{3+}$ ;  $n = 3$  or 4) [16],  $[\text{M}(\text{NCS})_4]^{2-}$  ( $\text{M} = \text{Co}^{2+}$ ,  $\text{Mn}^{2+}$ ,  $\text{Zn}^{2+}$ ) [17–19], and  $[\text{MX}_4]^{2-}$  ( $\text{M} = \text{Co}^{2+}$ ,  $\text{Mn}^{2+}$ ,  $\text{Cu}^{2+}$ ,  $\text{X} = \text{Cl}$ ,  $\text{Br}$ ) [20–22], the weak non-covalent cation-cation, anion-anion, and anion-cation interactions contribute considerably to stabilize conformations and result in the generation of novel magnetic, electrical, optical, and catalytic properties. Our research interest has recently been focused on the preparation of more suitable counterions to tune the crystal stacking structure of above-mentioned anions with a view to obtaining new inorganic-organic hybrid materials. Recent examples involving structural and magnetic data include  $[\text{4RBzDMAP}]_2[\text{Cu}(\text{mnt})_2]$  ( $\text{R} = \text{F}$ ,  $\text{Cl}$  and  $\text{Br}$ ,  $[\text{BzDMAP}]^+ = 1\text{-benzyl-4'-dimethylaminopyridinium}$ ) [23],  $[\text{1-NaMePid}][\text{Ni}(\text{mnt})_2]$  and  $[\text{2-NaMePid}][\text{Ni}(\text{mnt})_2]$  ( $[\text{NaMePid}]^+ = 1\text{-naphthylmethylpiperidinium}$ ) [24],  $[\text{BzTPP}]_2[\text{Co}(\text{NCS})_4]$  and  $[\text{4NO}_2\text{BzTPP}]_2[\text{Co}(\text{NCS})_4]$  ( $[\text{BzTPP}]^+ = \text{benzyltriphenylphosphonium}$ ) [25],  $[\text{4RBzPy}]_2\text{CuCl}_4$  ( $\text{R} = \text{Cl}$ ,  $\text{NO}_2$ ;  $[\text{BzPy}]^+ = \text{benzylpyridinium}$ ) [26]. In order to widen our research, we have firstly introduced  $[\text{4NO}_2\text{BzPy}]^+$  into the system containing the  $[\text{Co}(\text{NCS})_4]^{2-}$

anion and obtained a new ion-paired compound:  $[4\text{NO}_2\text{BzPy}]_2[\text{Co}(\text{NCS})_4]$  (**1**). Their spectra, crystal structures, and magnetic properties have been investigated.

## EXPERIMENTAL

**Synthesis.**  $[4\text{NO}_2\text{BzPy}]_2[\text{Co}(\text{NCS})_4]$  (**1**) was prepared by a direct combination of 2:1:4 mol equiv of  $[4\text{NO}_2\text{BzPy}]_{\text{Br}}$ ,  $\text{CoCl}_2$  and  $\text{KSCN}$  in methanol. A blue precipitate given was filtered off, washed with cool ether, and dried under vacuum with a yield of 78 %. Blue block crystals suitable for the X-ray diffraction analysis were obtained from  $\text{CH}_3\text{CN}$  by slow evaporation of the solvent of complex **1** for about two weeks. Anal. Calcd. for  $\text{C}_{28}\text{H}_{22}\text{N}_8\text{O}_4\text{S}_4\text{Co}$  (%): C, 46.60; H, 3.07; N, 15.53. Found: C, 46.56; H, 3.12; N, 15.46. IR (KBr,  $\text{cm}^{-1}$ ): 3049(w), 3025(w), 2922(w), 2851(w), 2062(vs), 1632(m), 1521(s), 1482(m), 1347(s), 1280(w), 1169(w), 1114(w), 854(m), 767(s). UV-Vis spectrum (nm) (lg $\epsilon$ ): 259(6.23), 316(5.60), 628(4.70). Pyridine, 4-nitrobenzyl bromide,  $\text{CoCl}_2 \cdot 6\text{H}_2\text{O}$ , and  $\text{KSCN}$  were purchased from Aldrich Chemical Company and used without purification. 1-(4'-Nitrobenzyl)pyridinium bromide ( $[4\text{NO}_2\text{BzPy}]_{\text{Br}}$ ) was synthesized following the published procedures [27]. All other reagents were commercially available and used as received. Combustion analyses (C, H, N) were performed on a Perkin Elmer 240C Elemental Analyzer. The IR spectrum (KBr pellets) was recorded on a Nicolet AVATAR 360 spectrophotometer in the range  $4000\text{--}400\text{cm}^{-1}$ . The electrospray mass spectrum [ESI-MS] of a MeCN solution of the complex was obtained with a Finnigan LCQ mass spectrometer. The UV-visible spectrum of the complex in HPLC grade  $\text{CH}_3\text{CN}$  in the range 200–800 nm was recorded on a Shimadzu UV-2500 spectrophotometer in 1 cm quartz cells.

**Single crystal XRD.** Intensity data were collected on a Bruker SMART APEX CCD diffractometer employing  $\text{MoK}_{\alpha}$  radiation ( $\lambda = 0.71073\text{\AA}$ ) and graphite monochromatized  $\text{MoK}_{\alpha}$  radiation. Data collection, cell refinement, and data reduction were performed using the SHELXL-2000 program [28]. The structure was solved by direct methods and expanded via Fourier techniques. The non-hydrogen atoms were refined anisotropically by the full-matrix least-squares techniques. Hydrogen atoms were refined via a riding model with fixed isotropic U values. The CIF file with complete information about the structure was deposited with CCDC (No. 768800), from which it is available free of charge on request at [www.ccdc.cam.ac.uk/data\\_request/cif](http://www.ccdc.cam.ac.uk/data_request/cif). Crystallographic data:  $\text{C}_{28}\text{H}_{22}\text{N}_8\text{O}_4\text{S}_4\text{Co}$ ,  $M = 721.71$ , Orthorhombic,  $Pbcn$ ,  $a = 13.188(2)\text{\AA}$ ,  $b = 8.458(1)\text{\AA}$ ,  $c = 29.281(4)\text{\AA}$ ,  $V = 3266.2(7)\text{\AA}^3$ ,  $Z = 4$ ,  $D_{\text{calcd}} = 1.468\text{ g/cm}^3$ , 2871 reflections collected, 2357 independent reflections, full matrix least-squares on  $F^2$ , 204 parameters, final  $R$  indices [ $I = 2\sigma(I)$ ]:  $R1 = 0.0332$ ,  $wR2 = 0.0806$ . Selected bond lengths and bond angles are listed in Table 1.

**Magnetic susceptibility.** Magnetic data were collected using a Quantum Design MPMS-XL superconducting quantum interference device (SQUID) magnetometer. 0.0313 g of the powdered sample of **1** used in magnetic studies was prepared from crushed single crystals. The sample was packed into a small gelatin capsule and the temperature-dependent magnetic susceptibility data were collected over a temperature range 2–300 K at an applied magnetic field of 2 kOe. Diamagnetic correction was made with Pascal's constants for all constituent atoms, and the temperature-independent paramagnetic (TIP) correction for the cobalt atom was applied to the data sets.

Table 1

Selected bond lengths ( $d$ ,  $\text{\AA}$ ) and bond angles ( $\omega$ , deg.) for **1**

Bond	$d$	Bond	$d$	Angles	$\omega$	Angles	$\omega$
$\text{Co}(1)-\text{N}(1)$	1.959(2)	$\text{N}(2)-\text{C}(2)$	1.156(3)	$\text{N}(1)-\text{Co}(1)-\text{N}(2)$	105.03(8)	$\text{N}(3)-\text{C}(9)-\text{C}(8)$	113.2(2)
$\text{Co}(1)-\text{N}(2)$	1.961(2)	$\text{N}(3)-\text{C}(9)$	1.490(3)	$\text{Co}(1)-\text{N}(1)-\text{C}(1)$	160.27(18)	$\text{N}(3)-\text{C}(11)-\text{C}(10)$	120.4(2)
$\text{S}(1)-\text{C}(1)$	1.619(2)	$\text{N}(3)-\text{C}(10)$	1.332(3)	$\text{Co}(1)-\text{N}(2)-\text{C}(2)$	166.21(18)	$\text{O}(1)-\text{N}(4)-\text{O}(2)$	124.7(3)
$\text{S}(2)-\text{C}(2)$	1.611(2)	$\text{O}(1)-\text{N}(4)$	1.226(4)	$\text{S}(1)-\text{C}(1)-\text{N}(1)$	178.5(2)	$\text{O}(2)-\text{N}(4)-\text{C}(5)$	118.4(2)
$\text{N}(1)-\text{C}(1)$	1.161(3)	$\text{O}(2)-\text{N}(4)$	1.217(3)	$\text{S}(2)-\text{C}(2)-\text{N}(2)$	179.0(2)	$\text{O}(1)-\text{N}(4)-\text{C}(5)$	118.4(2)

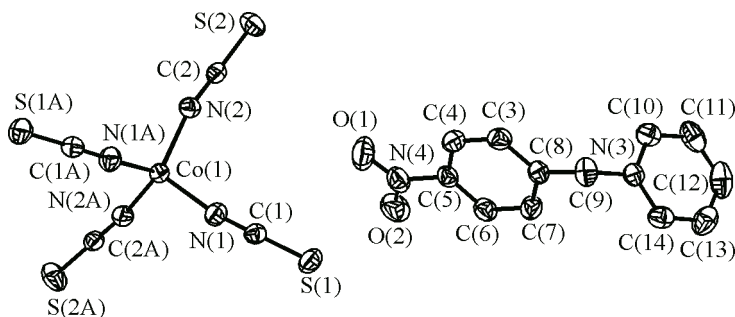


Fig. 1. ORTEP plot (30 % probability ellipsoids) showing the molecular structure of **1**

## RESULTS AND DISCUSSION

The bands at  $3049\text{ cm}^{-1}$ ,  $3025\text{ cm}^{-1}$ ,  $2922\text{ cm}^{-1}$ , and  $2851\text{ cm}^{-1}$  are due to the stretching vibrational frequencies of C—H in the aromatic ring and methylene. The very strong band at  $2062\text{ cm}^{-1}$  is the CN absorption of thiocyanate, which is indicative of bonding to the metal via the N atom, indeed, the CN absorption in ionic thiocyanate is such as in KNCS [29]. The bands at  $1631\text{ cm}^{-1}$  and  $1482\text{ cm}^{-1}$  are attributable to  $\nu(\text{C}=\text{N})$ ,  $\nu(\text{C}=\text{C})$  stretching bands for the phenyl and pyridinium rings. The bands at  $1521\text{ cm}^{-1}$  and  $1347\text{ cm}^{-1}$  for **1** are the  $\nu(\text{Ar}-\text{NO}_2)$  bands. The  $\delta(\text{C}-\text{H})$  bands of the phenyl and pyridinium rings are at  $854\text{ cm}^{-1}$  and  $767\text{ cm}^{-1}$ . The UV-Vis absorption spectra of **1** in the HPLC grade  $\text{CH}_3\text{CN}$  solvent in the range  $200$ — $800\text{ nm}$  were recorded. The band at  $259\text{ nm}$  is attributed to a  $\pi-\pi$  transition of the cationic portion of the complex; the band at  $316\text{ nm}$  is due to the charge transfer transition of the anionic portion, while the broad band observed at  $628\text{ nm}$  is a  $d-d$  transition band of the Co(II) ion, which are similar to these of the complex containing the  $[\text{Co}(\text{NCS})_4]^{2-}$  anion [30]. The positive-ion ESI-MS spectra of **1** in the  $\text{CH}_3\text{CN}$  solution show that the mass spectrum dominated by the  $215.2$  peak is due to  $[\text{4NO}_2\text{BzPy}]^{2+}$ .

$[\text{4NO}_2\text{BzPy}]_2[\text{Co}(\text{NCS})_4](\mathbf{1})$  crystallizes in the orthorhombic system with the space group  $Pbcn$ , and an asymmetric unit in a cell consists of half of a  $[\text{Co}(\text{NCS})_4]^{2-}$  anion and one  $[\text{4NO}_2\text{BzPy}]^+$  cation as shown in Fig. 1. The selected bond distances and angles are shown in Table 1. For  $[\text{Co}(\text{NCS})_4]^{2-}$  the coordination geometry of the central Co(II) ion could be described as a slightly distorted tetrahedron, and the  $\text{Co}(1)-\text{N}(1)$  and  $\text{Co}(1)-\text{N}(2)$  bond distances are  $1.959\text{ \AA}$  and  $1.961\text{ \AA}$ , and the  $\text{N}(1)-\text{Co}(1)-\text{N}(1)$  bond angle is  $105.03^\circ$ . These values are in good agreement with those found in the complexes containing the  $[\text{Co}(\text{NCS})_4]^{2-}$  anion [17—19, 25]. In the  $[\text{4NO}_2\text{BzPy}]^+$  cation, the N atom and two O atoms from the nitro group are tipped out of the phenyl planes with the deviations of  $-0.024\text{ \AA}$  for the N(4) atom,  $-0.178\text{ \AA}$  for the O(1) atom,  $0.116\text{ \AA}$  for the O(2) atom. The  $[\text{4NO}_2\text{BzPy}]^+$  cation adopts a conformation where both phenyl and pyridine rings are twisted relative to the  $\text{C}(8)-\text{C}(9)-\text{N}(3)$  reference plane with the dihedral angles to that plane of  $134.1^\circ$  and  $71.8^\circ$  respectively. The phenyl and pyridine rings are inclined at  $82.4^\circ$  to one another. It is interesting that  $\text{S}\cdots\text{Co}$  and  $\text{S}\cdots\text{N}$  interactions were observed between the adjacent  $[\text{Co}(\text{NCS})_4]^{2-}$  anions: (1) the short  $\text{S}(1)\cdots\text{Co}(1^i)$  (symmetry code:  $i = x, y+1, z$ ) interactions with the distances of  $3.626\text{ \AA}$ ; (2) the short  $\text{S}(1)\cdots\text{N}(2^{ii})$  (symmetry code:  $ii = -x+1, -y-1, -z$ ) interactions with the distances of  $3.227\text{ \AA}$ . These short interactions are similar to the short  $\text{S}\cdots\text{S}$  [2, 3, 31] or  $\text{C}\cdots\text{N}$  interactions [32—34] and result in the formation of a 2D layer structure of  $[\text{Co}(\text{NCS})_4]^{2-}$  anions (Fig. 2). It is noted that the  $[\text{4NO}_2\text{BzPy}]^+$  cations stack into a 1D column (Fig. 3a) by the  $\text{p}\cdots\pi$  stacking interaction [35, 36] between O(1) of one cation and the phenyl ring of another cation with a centroid-centroid distance of  $3.591\text{ \AA}$  (Fig. 3), and the columns are linked by the  $\text{C}-\text{H}\cdots\text{O}$  hydrogen bonds with a  $\text{C}\cdots\text{O}$  distance of  $3.267\text{ \AA}$ . The effect of the combination of weak hydrogen bonds, short  $\text{S}\cdots\text{Co}$  and  $\text{S}\cdots\text{N}$  interactions consolidate the crystal packing and generates a 3D structure (Fig. 4).

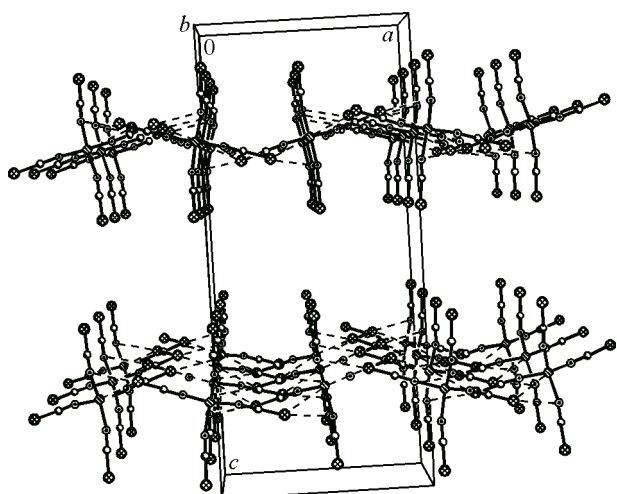


Fig. 2. Layer structure of  $[\text{Co}(\text{NCS})]^{2-}$  anions formed by  $\text{S}\cdots\text{N}$  and  $\text{S}\cdots\text{Co}$  interactions of **1**

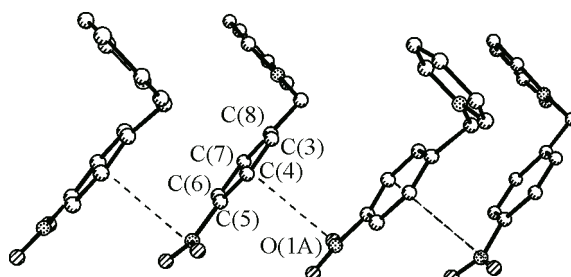


Fig. 3. 1D column formed by the  $p\cdots\pi$  interactions between the  $[\text{4NO}_2\text{BzPy}]^+$  cations of **1**

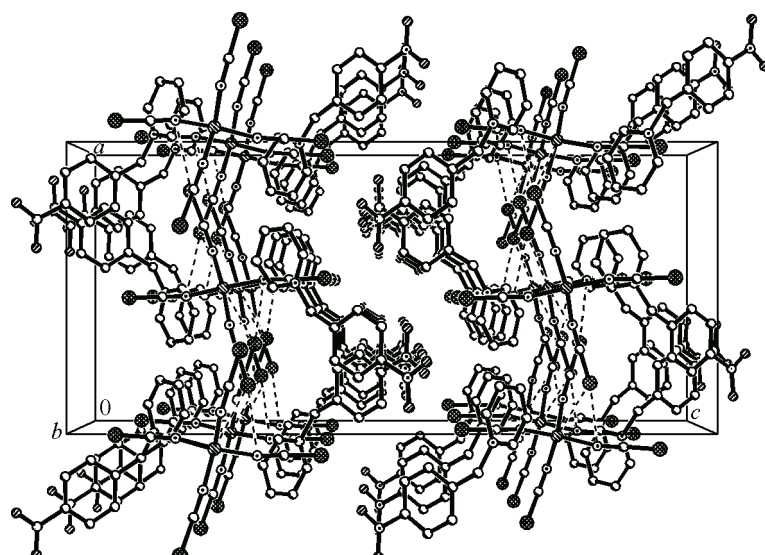


Fig. 4. Packing diagram of **1**

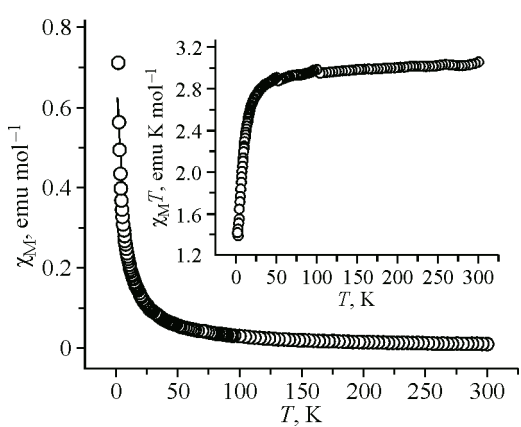


Fig. 5. Plot of  $\chi_M$  versus  $T$  for **1** (inset: plot of  $\chi_M T$  versus  $T$ ). The red solid line is reproduced from the theoretical calculations and detailed fitting procedure described in the text

The temperature dependence of the solid-state magnetic susceptibilities of **1** was investigated in the range 2—300 K under an applied field of 2000 Oe. As shown in Fig. 5, at 300 K the  $\chi_M T$  value is 3.055 emu·K·mol<sup>-1</sup>, which is larger than the spin-only value of high-spin Co(II) ( $S = 3/2$ ), 1.875 emu·K·mol<sup>-1</sup>, indicating a contribution of the orbital momentum typical of the  $^4T_{1g}$  ground state [37, 38]. As the temperature is lowered, the  $\chi_M T$  value of **1** slightly decreases to 2.731 emu·K·mol<sup>-1</sup> at 25 K, and drops to 1.421 emu·K·mol<sup>-1</sup> at 2 K, which is indicative of a weak antiferromagnetic exchange. The magnetic susceptibility data in the range 2—300 K can be finely fitted to the Curie-Weiss law (the solid line in the inset in Fig. 5) with  $C = 2.76$  emu·K·mol<sup>-1</sup>,  $\theta = -2.42$  K and  $R = 1.3 \times 10^{-4}$  ( $R$  is the agreement factor defined as  $\sum (\chi_M^{\text{calcd}} - \chi_M^{\text{obsd}})^2 / (\chi_M^{\text{obsd}})^2$ ).

This work has been partially supported by the Science and Technology Project (No. 2011B080701026, No. 2012B010200041) from the Guangdong Science and Technology Department and the key Academic Program of the 3rd phase "211 Project" of South China Agricultural University (No. 2009B010100001), and the university students' innovative experimental project (No. 201310564047) from the Education Department of Guangdong Province.

#### REFERENCES

1. Hollingsworth M.D. // Science. – 2002. – **295**. – P. 2410.
2. Bleiholder C., Werz D.B., Köppel H., Gleiter R. // J. Amer. Chem. Soc. – 2006. – **128**. – P. 2666.
3. Bleiholder C., Gleiter R., Werz D.B., Köppel H. // Inorg. Chem. – 2007. – **46**. – P. 2249.
4. Janiak C. // J. Chem. Soc., Dalton Trans. – 2000. – P. 3885.
5. Real J.A., Andres E., Munoz M.C., Julve M., Granier T., Bousseksou A., Varret F. // Science. – 1995. – **268**. – P. 265.
6. Jung O.S., Park S.H., Kim K.M., Jang H.G. // Inorg. Chem. – 1998. – **37**. – P. 5781.
7. Nishijo J., Ogura E., Yamaura J., Miyazaki A., Enoki T., Takano T., Kuwatani Y., Iyoda M. // Solid State Commun. – 2000. – **116**. – P. 661.
8. Akutagawa T., Nakamura T. // Coord. Chem. Rev. – 2002. – **226**. – P. 3.
9. Mukai K., Hatanaka T., Senba N., Nakayashiki T., Misaki Y., Tanaka K., Ueda K., Sugimoto T., Azuma N. // Inorg. Chem. – 2002. – **41**. – P. 5066.
10. Robertson N., Cronin L. // Coord. Chem. Rev. – 2002. – **227**. – P. 93.
11. Rovira C. // Chem. Eur. J. – 2000. – **6**. – P. 1723.
12. Coomber A.T., Beljonne D., Friend R.H., Brédas J.L., Charlton A., Robertson N., Underhill A.E., Kurmoo M., Day P. // Nature. – 1996. – **380**. – P. 144.
13. Huang Q., Liu J.F., Zuo H.R., Zhou J.R., Hou Y., Ni C.L., Meng Q.J. // Inorg. Chim. Acta. – 2009. – **362**. – P. 2461.
14. Ni Z.P., Ren X.M., Ma J., Xie J.L., Ni C.L., Chen Z.D., Meng Q.J. // J. Amer. Chem. Soc. – 2005. – **127**. – P. 14330.
15. Duan H.R., Ren X.M., Meng Q.J. // Coord. Chem. Rev. – 2010. – **254**. – P. 1509.
16. Ohba M., Okawa H. // Coord. Chem. Rev. – 2000. – **198**. – P. 313.
17. Chen H.J., Zhang L.Z., Cai Z.G., Yang G., Chen X.M. // J. Chem. Soc. Dalton Trans. – 2000. – 2463.
18. Skorupa A., Korybut-Daszkiewicz B., Mrozninski J. // Inorg. Chim. Acta. – 2001. – **325**. – P. 286.
19. Ghazzali M., Langer V., Öhrström L. // J. Solid. State. Chem. – 2008. – **181**. – P. 2191.
20. Herringer S.S., Turnbull M.M., Landee C.P., Wikaira J.L. // J. Coord. Chem. – 2009. – **62**. – P. 863.
21. Wikaira J.L., Li L.-X., Butcher R., Fitchett C.M., Jameson G.B., Landee C.P., Turnbull M.M. // J. Coord. Chem. – 2010. – **63**. – P. 2949.
22. Han S., Liang L.B., Chen W.Q., Liu J.F., Zhou J.R., Yang L.M., Ni C.L. // J. Coord. Chem. – 2011. – **64**. – P. 4182.
23. Huang Q., Lin J.H., Liang L.B., Chen X., Zuo H.R., Zhou J.R., Yang L.M., Ni C.L., Hu X.L. // Inorg. Chim. Acta. – 2010. – **363**. – P. 2546.
24. Zhou J.R., Chen X., Hou Y., Zheng Y.P., Huang Q., Zuo H.R., Yang L.M., Ni C.L., Meng Q.J. // Synth. Met. – 2010. – **160**. – P. 797.
25. Chen X., Chen W.Q., Han S., Liu J.F., Zhou J.R., Yu L.L., Yang L.M., Ni C.L., Hu X.L. // J. Mol. Struct. – 2010. – **984**. – P. 164.
26. Han S., Cai Z.F., Xiong Y.H., Huang Q., Zheng Y., Zhou J.R., Liu X.P., Yang L.M., Ni C.L. // Inorg. Chim. Acta. – 2011. – **379**. – P. 140.

27. Bulgarevich S.B., Bren D.V., Movshovic D.Y., Finocchiaro P., Failla S. // J. Mol. Struct. – 1994. – **317**. – P. 147.
28. SHELXTL, Version 5.10. Structure determination software programs, Bruker Analytical X-ray Systems Inc. Madison. Wisconsin, USA, 2000.
29. Nakamoto K. Infrared and Raman spectra of inorganic and coordination compound. 3rd Ed. – New York: Wiley, 1978.
30. Banerjee S., Ray A., Sen S., Mitra S., Hughes D.L., Butcher R.J., Stuart R., Batten S.R., Turner D.R. // Inorg. Chim. Acta. – 2008. – **361**. – P. 2692.
31. Steiner T. // Angew. Chem. Int. Ed. – 2002. – **41**. – P. 48.
32. Zuo H.R., Huang Q., Huang C.Y., Huang D.H., Hou Y., Yang L.M., Ni C.L., Meng Q.J. // J. Solid State Chem. – 2009. – **182**. – P. 147.
33. Zuo H.R., Wu L.X., Huang Q., Chen X., Zhou J.R., Yang L.M., Ni C.L., Hu X.L. // Inorg. Chim. Acta. – 2009. – **362**. – P. 3657.
34. Huang Q., Hou Y., Zhu H.M., Zhou J.R., Zuo H.R., Ni C.L., Meng Q.J., Hu X.L. // J. Coord. Chem. – 2009. – **62**. – P. 2012.
35. Ren X.M., Meng Q.J., Song Y., Lu C.S., Hu C.J. // Inorg. Chem. – 2002. – **41**. – P. 5686.
36. Wan C.Q., Li X., Wang C.Y., Qiu X. // J. Mol. Struct. – 2009. – **930**. – P. 32.
37. Wei Y., Wu K., Broer R., Zhuang B., Yu Y. // Inorg. Chem. Commun. – 2007. – **10**. – P. 910.
38. Li B.L., Wang X.Y., Zhu X., Gao S., Zhang Y. // Polyhedron. – 2007. – **26**. – P. 5219.